

Temporal variations and spectral properties of the Be/X-ray pulsar GRO J1008–57 studied by INTEGRAL *

Wei Wang

National Astronomical Observatories, Chinese Academy of Sciences, Beijing 100012, China;
wangwei@bao.ac.cn

Received 2013 August 29; accepted 2013 December 19

Abstract The spin period variations and hard X-ray spectral properties of the Be/X-ray pulsar GRO J1008–57 are studied with INTEGRAL observations during two outbursts in 2004 June and 2009 March. The pulsation periods of ~ 93.66 s in 2004 and ~ 93.73 s in 2009 are determined. Pulse profiles of GRO J1008–57 during outbursts are strongly energy dependent with a double-peaked profile from 3–7 keV and a single-peaked profile in hard X-rays above 7 keV. Combined with previous measurements, we find that GRO J1008–57 has undergone a spin-down trend from 1993 – 2009 with a rate of $\sim 4.1 \times 10^{-5} \text{ s d}^{-1}$, and could have changed into a spin-up trend after 2009. We find a relatively soft spectrum in the early phase of the 2009 outburst with cutoff energy ~ 13 keV. Above a hard X-ray flux of $\sim 10^{-9} \text{ erg cm}^{-2} \text{ s}^{-1}$, the spectra of GRO J1008–57 during outbursts need an enhanced hydrogen absorption with column density $\sim 6 \times 10^{22} \text{ cm}^{-2}$. The observed dip-like pulse profile of GRO J1008–57 in soft X-ray bands could be caused by this intrinsic absorption. Around the outburst peaks, a possible cyclotron resonance scattering feature at ~ 74 keV is detected in the spectra of GRO J1008–57 which is consistent with the feature that was reported in MAXI/GSC observations, making the source a neutron star with the highest known magnetic field ($\sim 6.6 \times 10^{12}$ G) among accreting X-ray pulsars. This marginal feature is supported by the present detections in GRO J1008–57 following the correlation between the fundamental line energies and cutoff energies in accreting X-ray pulsars. Finally we discovered two modulation periods at ~ 124.38 d and ~ 248.78 d using RXTE/ASM light curves of GRO J1008–57. Two flare peaks appearing in the folded light curve had different spectral properties. The normal outburst lasting 0.1 of an orbital phase had a hard spectrum and could not be significantly detected below 3 keV. The second flare lasting ten days showed a very soft spectrum without significant detections above 5 keV. GRO J1008–57 is a good candidate of an accreting system with an equatorial circumstellar disk around the companion star. The neutron star passing the disk of the Be star near periastron and apastron produces two X-ray flares. The soft spectral properties in the secondary flares still need further detailed studies with soft X-ray spectroscopy.

Key words: stars: individual (GRO J1008–57) — stars: neutron — stars: magnetic fields — binaries: close — X-rays: binaries

* Supported by the National Natural Science Foundation of China.

1 INTRODUCTION

The Be/X-ray pulsar GRO J1008–57 was discovered by the BATSE experiment aboard the Compton Gamma Ray Observatory during its 1993 outburst (Stollberg et al. 1993). This source has shown periodic outbursts that were detected by different X-ray missions during the last 20 yr. These X-ray outburst activities are classified as Type I outbursts, which could be distinguished by their orbital period. In the BATSE era, the outbursts were detected during 1993 August, 1994 March, 1994 November and 1996 March, and occurred at multiples of ~ 248 d, which indicates that this may be the orbital period of the system (Bildsten et al. 1997). Shrader et al. (1999) analyzed the light curve collected over three years of RXTE/ASM monitoring data, and suggested an orbital period of ~ 136.5 d. Also, Levine & Corbet (2006) re-analyzed the RXTE/ASM monitoring data of GRO J1008–57 from 1996–2005, and detected an orbital period of ~ 248.9 d. Independent analysis of variations in the pulse period of the X-ray pulsar in GRO J1008–57 during outbursts using the BATSE data estimated an orbital period of ~ 247.8 d (Coe et al. 2007). Using the available RXTE, Swift and Suzaku data from previous outbursts of GRO J1008–57, Kühnel et al. (2013) derived an orbital period of ~ 249.46 d using the pulse arrival time of the X-ray pulsar.

The pulse period of GRO J1008–57 was clearly detected during its discovery in 1993 August. X-ray pulsations with a period of ~ 93.587 s were detected in 20–120 keV band light curves of the pulsar obtained from BATSE observations (Stollberg et al. 1993). Using ROSAT observations of the pulsar during the same X-ray outburst, ~ 93.4 s pulsations with a double-peaked pulse profile were detected in 0.1–2.4 keV light curves (Petre & Gehrels 1994). The double-peaked pulse profile with a period of ~ 93.62 s was also detected by ASCA (Shrader et al. 1999) during the 1993 outburst, and above 10 keV in the energy range of BATSE; it evolved to a single-peaked profile. The spin period of the X-ray pulsar GRO J1008–57 may undergo a spin-up/spin-down trend. During an outburst in 2007, a pulsation period at ~ 93.73 s was detected by Suzaku (Naik et al. 2011). Kühnel et al. (2013) derived the spin period at 93.6793 ± 0.0002 s during the 2005 outburst and of $\sim 93.7134 \pm 0.0002$ s during the 2007 outburst. In a recent outburst in 2012, a pulsation period of ~ 93.648 s was found by Swift observations (Kühnel et al. 2013). Yamamoto et al. (2013) detected X-ray pulsations at ~ 93.6257 s in GRO J1008–57 using a Suzaku observation of the pulsar in 2012 November. These variations in the spin period are larger than the effect caused by its orbital period (less than ~ 0.03 s), suggesting that this source may undergo long-term variations in spin period.

In general, Be/X-ray pulsar systems have a magnetized neutron star with a magnetic field $> 10^{12}$ G, according to detections of a cyclotron resonance scattering feature (CRSF) in several cases, such as 4U 0115+63 (Li et al. 2012) and GX 304-1 (Klochkov et al. 2012). The X-ray spectra of GRO J1008–57 from different observations have not shown significant absorption features. Shrader et al. (1999) combined the ASCA and BATSE data to obtain a broadband spectrum from 1–150 keV during the 1993 outburst, detecting a marginal absorption feature around 88 keV, and suggested that the fundamental line energy may be about 44 keV. Suzaku observations of the pulsar during the 2007 November–December X-ray outburst, however, did not show the presence of any absorption feature in the spectrum in the 0.2–60 keV energy range (Naik et al. 2011). Yamamoto et al. (2013) reported a possible absorption feature around 76 keV during the 2012 outburst by using Suzaku/PIN (15–70 keV) and MAXI/GSC (60–140 keV) observations. As there was no absorption feature in the spectrum at low energy (i.e. ~ 40 keV), they suggested that GRO J1008–57 may be the neutron star with the highest magnetic field ($\sim 6.6 \times 10^{12}$ G) among known binary X-ray pulsars. Recently, Kühnel et al. (2013) found a possible absorption feature around 88 keV during the 2007 outburst with RXTE/HEXTE and Suzaku/GSO. This feature is similar to the feature that was reported with BATSE, but inconsistent with the result by MAXI/GSC. Thus, further observations and broadband spectral studies of this source in X-ray are still needed.

INTEGRAL observed GRO J1008–57 during two outbursts in 2004 June and 2009 March, respectively. With a broad observational energy range spanning 3–200 keV, INTEGRAL can con-

strain the hard X-ray spectral properties of GRO J1008–57 well, providing a good chance to search for CRSFs. The INTEGRAL observations are briefly introduced in the next section, Section 2. In Section 3, the spin period of GRO J1008–57 during the outburst is derived, and the long-term variation in spin period is found. In addition, the orbital modulation properties of this source are also studied with the available RXTE/ASM data. In Section 4, the hard X-ray spectral properties in different luminosity ranges are analyzed in detail by INTEGRAL, with the main aim of searching for possible CRSFs. Finally, the conclusion and discussion are presented in Section 5.

2 INTEGRAL OBSERVATIONS

INTEGRAL observed the hard X-ray transient GRO J1008–57 during two outbursts that occurred in 2004 June and 2009 March (see Fig. 1). We mainly use the data collected with the low-energy array called Imager on Board the INTEGRAL Satellite (IBIS), which incorporates a coded mask for imaging called INTEGRAL Soft Gamma-Ray Imager (ISGRI), (Lebrun et al. 2003). IBIS/ISGRI has a $12'$ (FWHM) angular resolution and source location accuracy of $\sim 1'$ in the energy band 15–200 keV. JEM-X, a small X-ray detector onboard INTEGRAL (Lund et al. 2003), collects the lower energy photons from 3–35 keV, which are used to constrain properties of the soft X-ray band of GRO J1008–57 combined with IBIS.

During the outburst in 2004 June, GRO J1008–57 was observed by INTEGRAL in three satellite orbital revolutions (one revolution ~ 3 d), whereas during the outburst in 2009 March, INTEGRAL observations of the source were available for four revolutions. In Table 1, the available INTEGRAL

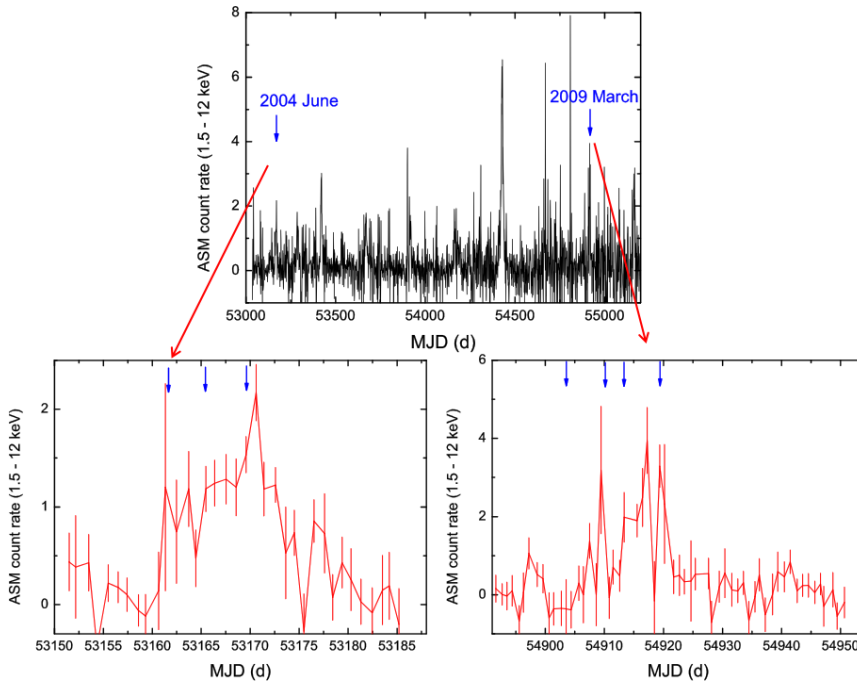


Fig. 1 Dates when the INTEGRAL observations were taken versus the RXTE/ASM count rate from 2004–2009. The INTEGRAL observations were performed during two outbursts in 2004 June and 2009 March, respectively (as noted by the arrows).

Table 1 INTEGRAL/IBIS observations of the field around GRO J1008–57 within the off-axis angle below 10° during two intervals of time in 2004 June and 2009 March. The time intervals of the observations in the revolution number and the corresponding MJD dates, and the corrected on-source exposure times are listed. The mean IBIS count rates and the significance level of the detection in the energy range 20–70 keV are also shown.

Rev.	Obs Date (MJD)	IBIS rate	Detection significance level (σ)	On-source time (ks)
201	53161.87–53164.37	1.47 ± 0.06	25	177
202	53165.34–53167.42	3.01 ± 0.07	43	136
203	53168.01–53170.09	6.10 ± 0.07	87	122
783	54903.79–54905.07	0.82 ± 0.10	8	100
785	54911.05–54911.99	0.96 ± 0.12	8	76
786	54913.19–54914.04	8.75 ± 0.12	72	69
788	54919.20–54920.02	15.53 ± 0.13	117	66

observations used in this paper are summarized. The archival data used in our work are available from the INTEGRAL Science Data Center.

The analysis is performed using the standard INTEGRAL off-line scientific analysis (OSA, Goldwurm et al. 2003) software, version 10. The bad science windows during solar activity and soon after the perigee passage are removed from our analysis. Individual pointings in each satellite revolution, processed with OSA 10, are mosaicked to create sky images for the source detection. We used the energy range 20–70 keV by IBIS for source detection and the quoted source fluxes for each revolution (see Table 1). The data reduction process and background estimation are performed through the standard pipeline processing methods (see also Bird et al. 2010).

3 TIMING ANALYSIS

3.1 Long-term Evolution of Spin Period

INTEGRAL monitored GRO J1008–57 during two outbursts in 2004 and 2009 respectively. We will search for the spin period of this source in two outbursts, and then possible long-term variations in the spin period can be checked. The light curves after background subtraction for both detectors, JEM-X and IBIS, are derived for five revolutions during the outburst (Significance level higher than 20σ): 201, 202, 203, 786 and 788. The time resolution for each light curve is about ~ 3 s. Barycentric corrections have been carried out before searching for the spin period.

In Figure 2, the power spectra of the IBIS light curves from 20–70 keV are presented for four revolutions. We cannot find a strong periodic signal in the data from revolution 201. We derived the observed values of spin period for the other four revolutions using the HEASOFT software package *efsearch* and the technique of pulse folding. To estimate accurate values of spin period, the observed data were corrected for the orbital motion of the neutron star in the binary system. Using the orbital parameters provided by Kühnel et al. (2013), the observed spin period can be corrected to the intrinsic period for each observed time interval. The derived values of spin period for GRO J1008–57 in four revolutions are given in Table 2. The spin period of the pulsar was determined to be ~ 93.66 s and 93.73 s during the 2004 June and 2009 March outbursts, respectively. With INTEGRAL observations, the trend of a long-term change in spin period in GRO J1008–57 is found.

The pulse profiles in ranges 3–7, 7–20 and 20–70 keV, obtained from JEM-X and IBIS data for revolution 788, are presented in Figure 3. The pulse profiles are found to change with energy. At soft X-ray energy ranges (< 7 keV), the pulse profile appears to be double-peaked whereas at high energies (> 7 keV), it becomes a single-peaked profile. However, the pulsed fraction remains constant in all energy ranges.

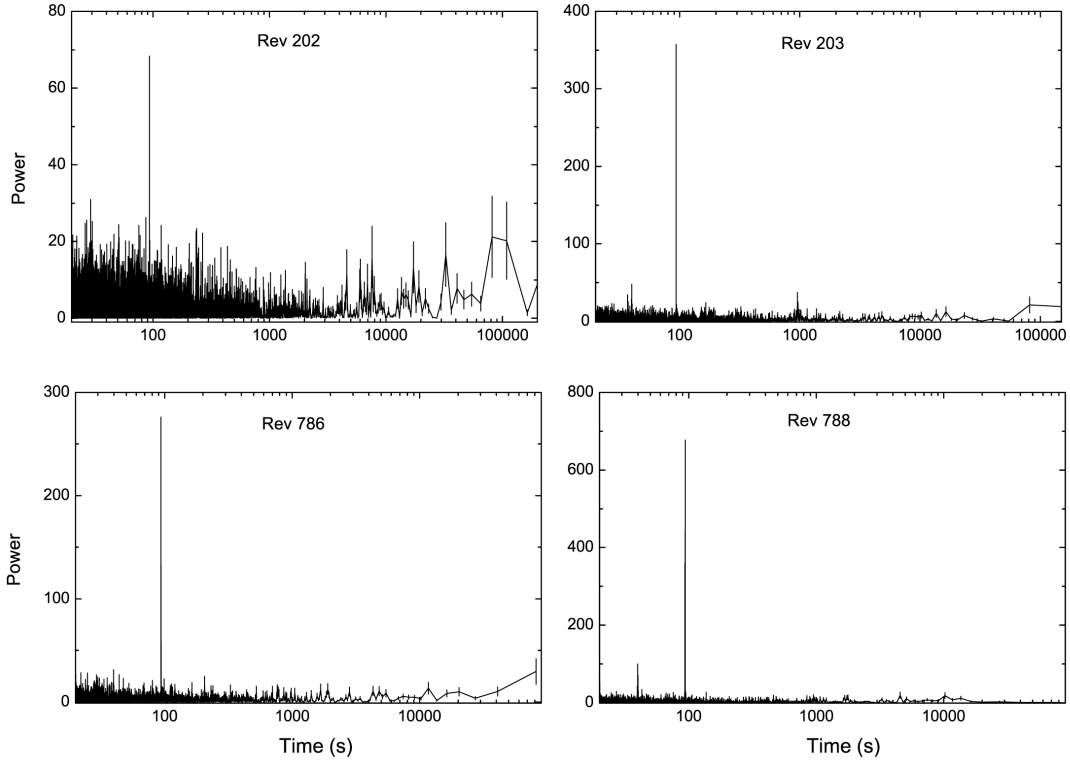


Fig. 2 The power spectra for the hard X-ray light curves from 20–70 keV obtained by IBIS for four revolutions: 202, 203, 786 and 788. A significant peak at ~ 93.7 s is detected in all spectra.

Table 2 The Spin Period of GRO 1008–57 according to Different Measurements

MJD	Spin Period (s)	Missions	References
49182	93.587 ± 0.015	BATSE	Stollberg et al. (1993)
49205	93.621 ± 0.011	ASCA	Shrader et al. (1999)
50176	93.55 ± 0.02	BATSE	Shrader et al. (1999)
53166	93.663 ± 0.006	INTEGRAL	This work
53168	93.664 ± 0.003	INTEGRAL	This work
53168	93.668 ± 0.001	INTEGRAL	Coe et al. 2007
53430	93.6793 ± 0.0002	RXTE	Kühnel et al. (2013)
54430	93.7134 ± 0.0002	RXTE	Kühnel et al. (2013)
54432	93.737 ± 0.001	Suzaku	Naik et al. (2011)
54912	93.733 ± 0.006	INTEGRAL	This work
54920	93.732 ± 0.005	INTEGRAL	This work
55658	93.727 ± 0.001	RXTE	Kühnel et al. (2013)
55917	93.722 ± 0.001	Swift	Kühnel et al. (2013)
56245	93.648 ± 0.002	Swift	Kühnel et al. (2013)
56251	93.6257 ± 0.0005	Suzaku	Yamamoto et al. (2013)

In Figure 4 and Table 2, we collected measurements of the spin period obtained by different missions in the past. All values of spin period were obtained during outbursts near the periastron passage of the neutron star. From the 1990s to 2009, GRO J1008–57 should have undergone a

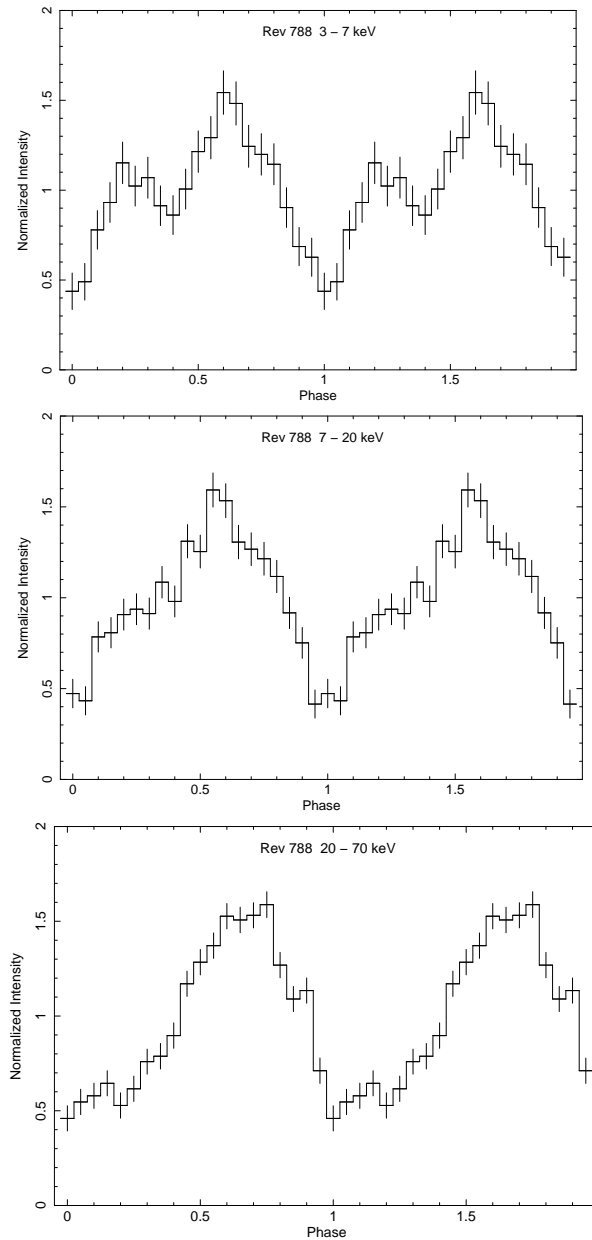


Fig. 3 The JEM-X and IBIS/ISGRI light curves of GRO J1008-57 after background subtraction for revolution 788 folded at a pulsation period (93.732 s) in three different energy ranges: 3–7, 7–20 and 20–70 keV. Double peaks appear in the light curves in the lower energy range of < 7 keV; above 7 keV, a single main peak is found in the hard X-ray light curves.

long-term spin-down trend, with the spin period varying from ~ 93.55 s to ~ 93.73 s. The average spin-down rate is given as $\sim (4.1 \pm 0.9) \times 10^{-5} \text{ s d}^{-1}$. But after 2009 (maybe around 2009–2011), the source changed to a long-term spin-up trend. The spin period changed from ~ 93.73 s in 2009 to ~ 93.63 s in 2012 December.

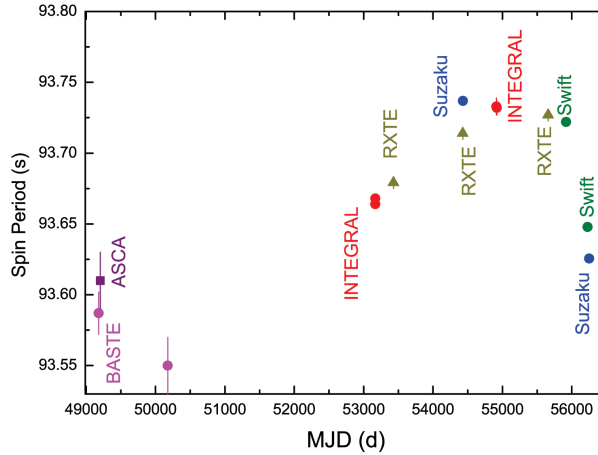


Fig. 4 The spin period of the neutron star in GRO J1008–57 determined by different measurements (data points taken from Table 2).

3.2 Orbital Modulations

The orbital period of GRO J1008–57 has been measured during the last 10 yr. Both the technique of pulse arrival time (Coe et al. 2007; Kühnel et al. 2013) and recurrence of hard X-ray outbursts (Bildsten et al. 1997; Levine & Corbet 2006) have shown the same value for orbital period of around 248 d. Using RXTE/ASM monitoring data, Shrader et al. (1999) reported the orbital period of GRO J1008–57 to be ~ 136 d. Using ~ 15 yr of RXTE/ASM data (1996–2011), we also study the characteristics of orbital modulation for GRO J1008–57.

In Figure 5, the power spectrum of the ASM light curve (averaged over one day) from 1.5–12 keV is displayed. The reported orbital period of ~ 248.78 d is clearly detected. Furthermore, along with the peak at ~ 248.78 d, another more significant peak appears at the period of ~ 124.38 d, which is half the orbital period of GRO J1008–57. What is the physical origin of this modulation period?

We folded the ASM light curve from 1.5–12 keV at the orbital period of 248.78 d, as shown in Figure 6. It is quite interesting that two peaks appear in the light curve from 1.5–12 keV. One peak, lasting about 0.1 orbital phases, is generally known as a type I outburst that coincides with the periastron passage of the neutron star. The other peak, separated by ~ 0.5 orbital phases from the normal outbursts, is weaker than the type I outbursts in the band 1.5–12 keV, and lasts about 10 d. RXTE/ASM has three energy bands: 1.5–3, 3–5 and 5–12 keV. Thus we also derived the hardness ratio of the light curve using two bands, 5–12 keV/1.5–3 keV, and folded it at the same orbital period. The folded hardness ratio versus orbital phases is also presented in Figure 6. The two flux peaks have quite different spectral properties: the type I outbursts show large values of hardness ratio, generally higher than 1, while the second peak has hardness ratios below 1.

Thus the outbursts showing the hard spectrum become a relatively weak peak in the 1.5–3 keV band, and sometimes cannot be clearly observed. The second peak has a very soft spectrum that would not be observed above 5 keV. We also checked the pointing observations by INTEGRAL in the time intervals covering or near the second peaks, but GRO J1008–57 could not be detected by either JEM-X or IBIS, also suggesting a very soft spectrum that may not be significantly detected above 3 keV. So, the hard X-ray detectors like BATSE, Swift and INTEGRAL could only detect the hard X-ray outburst events near the periastron, implying an orbital modulation of ~ 248.8 d.

However, in the softer X-ray monitoring by RXTE/ASM, a soft peak component appears near the apastron of the orbital phase. Then the modulation period at 124 d could be detected.

4 HARD X-RAY SPECTRAL PROPERTIES

INTEGRAL observations on GRO J1008–57 reported significant detections in seven revolutions from 2004 June and 2009 March. We extract the spectrum of both JEM-X and IBIS from each revolution. Then we fit the broad spectrum from 3–200 keV combined with the JEM-X and IBIS data. Generally, the spectrum of accreting X-ray pulsars like GRO J1008–57 can be described by a power-law model plus a high-energy exponential rolloff: $A(E) = KE^{-\Gamma} \exp(-E/E_{\text{cutoff}})$. Sometimes, spectra below 5 keV cannot be fitted well with a simple power law, so photoelectric absorption is then added to fit the spectra.

Cross-calibration studies on the JEM-X and IBIS/ISGRI detectors have been performed using observation data of the Crab pulsar, and the calibration between JEM-X and IBIS/ISGRI can be sufficiently good within $\sim 6\%$ (see the samples in Jourdain et al. 2008 and Wang 2013). In the spectral fittings, the constant factor between JEM-X and IBIS is set to be 1. The spectral analysis software package used is XSPEC 12.6.0q.

One revolution, which had an INTEGRAL observation, detected GRO J1008–57 just before the 2009 March outburst in the light curve of RXTE/ASM (Fig. 1). We define this revolution as the quiescent state when GRO J1008–57 also had a low significance level for the detection ($\sim 8\sigma$) by IBIS. For the other six revolutions, we define these as the outburst states. We will study the hard X-ray spectral properties in two states separately.

4.1 Quiescent States

INTEGRAL observed the hard X-ray transient source GRO J1008–57 just before the X-ray outburst detected by RXTE/ASM in 2009 March (see Fig. 1) in revolution 783. However, during quiescence, GRO J1008–57 was detected by both JEM-X and IBIS.

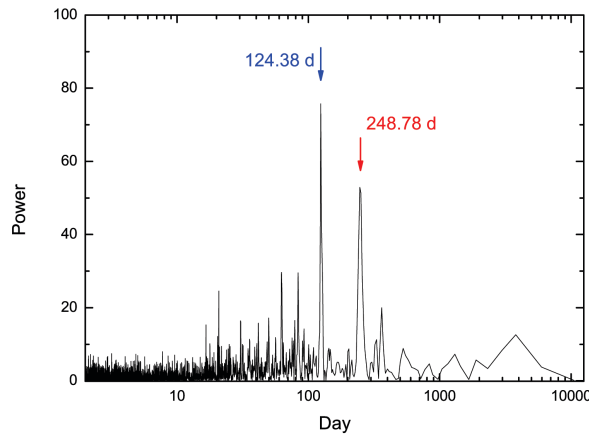


Fig. 5 The power spectrum of the RXTE/ASM light curves (1.5–12 keV), averaged over one day, on the source GRO J1008–57 from 1997–2011. Two significant peaks are detected, one at $\sim 248.78 \pm 0.29$ d and the other at $\sim 124.38 \pm 0.12$ d, which is half the former one. The 248.78 d value is thought to be the real orbital period of GRO J1008–57, and is consistent with the previous results (Coe et al. 2007; Levine & Corbet 2006).

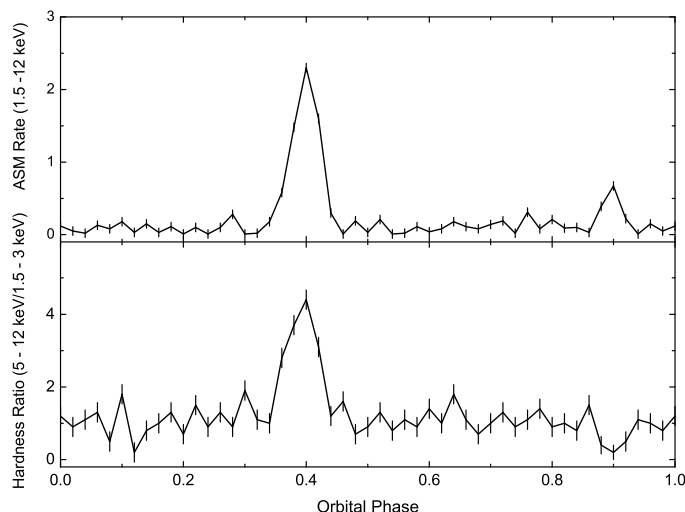


Fig. 6 *Top*: RXTE/ASM light curve (1.5–12 keV) of 4U 2206+54 folded at an orbital period of 248.78 d. The outburst peak around phase 0.4 and the second peak around phase 0.9 are found in the light curve. *Bottom*: Light curve showing the hardness ratio of two ASM energy bands, 5–12 keV/1.5–3 keV, folded at an orbital period of 248.78 d. The outburst peak shows the hardness ratio peak with the ratio > 1 , but the harness ratio of the second peak is lower than 1.

Table 3 Hard X-ray spectral parameters of GRO J1008–57 observed during seven revolutions. The flux is given in units of 10^{-9} erg cm^{-2} s^{-1} in the range of 3–100 keV and the column density (N_{H}) in units of 10^{22} cm^{-2} . For two revolutions, 203 and 788, the spectral parameters are presented with two different fits: no CRSF and with CRSF.

Rev. Number	N_{H}	Γ	E_{cutoff} (keV)	E_c (keV)	Width (keV)	Depth	Flux	χ^2 (d.o.f.)
201	–	1.57 ± 0.12	27.4 ± 5.8	–	–	–	0.34 ± 0.04	0.6739(64)
202	–	1.33 ± 0.07	23.2 ± 2.5	–	–	–	0.65 ± 0.05	1.029(95)
203 (no CRSF)	4.9 ± 1.1	1.29 ± 0.07	24.1 ± 1.9	–	–	–	1.24 ± 0.06	1.298(102)
203 (CRSF)	4.9 ± 1.1	1.34 ± 0.07	26.9 ± 1.9	74.1 ± 5.3	$< 10(2\sigma)$	$< 1.9(2\sigma)$	1.23 ± 0.06	0.8197(99)
783	–	2.09 ± 0.29	59.7 ± 22.9	–	–	–	0.22 ± 0.06	0.7288(15)
785	–	1.07 ± 0.33	13.2 ± 3.9	–	–	–	0.32 ± 0.07	1.068(17)
786	7.1 ± 1.5	1.55 ± 0.09	27.4 ± 2.8	–	–	–	1.81 ± 0.08	0.7824(99)
788 (no CRSF)	5.9 ± 1.1	1.38 ± 0.06	27.6 ± 1.6	–	–	–	3.11 ± 0.09	1.379(105)
788 (CRSF)	6.3 ± 1.1	1.44 ± 0.06	28.7 ± 2.1	73.4 ± 3.1	3.5 ± 1.9	1.7 ± 0.8	3.09 ± 0.09	0.8376(102)

In Figure 7, we present the spectrum of GRO J1008–57 from 3–100 keV. The spectrum is fitted with a cutoff power-law model, with a cutoff energy of $\sim 59.7 \pm 22.9$ keV. The large values of the cutoff energy and uncertainty suggest that the spectrum can be fitted by a simple power-law model. The power-law model gives a photon index of $\Gamma = 2.11 \pm 0.24$ with a reduced $\chi^2 \sim 0.8577$ (16 d.o.f.). The photon index of ~ 2.1 implies a generally harder spectrum than those of accreting X-ray pulsars. The hard X-ray flux from 3–100 keV is $\sim 2.2 \times 10^{-10}$ erg cm^{-2} s^{-1} , corresponding to a luminosity of $\sim 6 \times 10^{35}$ erg s^{-1} assuming a distance of 5 kpc, estimated by Coe et al. (1994).

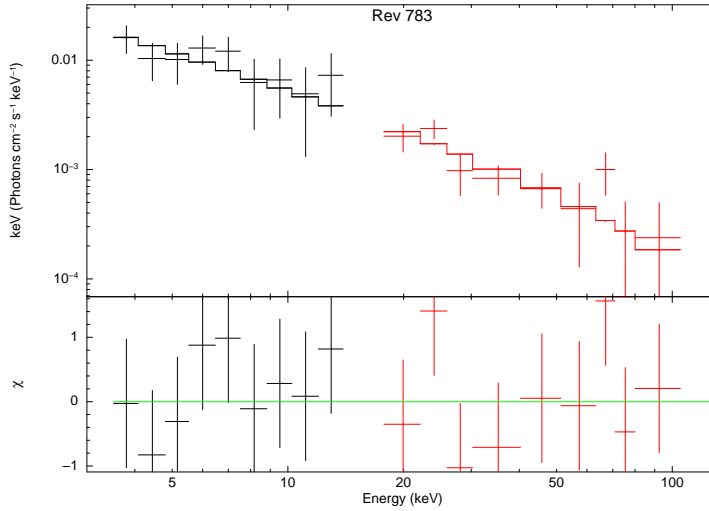


Fig. 7 The hard X-ray spectrum of GRO J1008–57 during the quiescent states obtained by JEM-X and IBIS in revolution 783 (see Table 3). The spectrum is fitted by a power-law plus high energy exponential rolloff, but the simple power-law model can also describe the spectrum well.

4.2 Outburst States

During the outbursts, six spectra for GRO J1008–57 were extracted by INTEGRAL observations. The spectra from 3–200 keV in six revolutions were well fitted by a cutoff power-law model (see Table 3, and Figs. 8 and 9). In revolution 785, IBIS detected the source at a low significance level ($\sim 8\sigma$), but in the ASM light curve, GRO J1008–57 had gone into the outburst phase. Combined with JEM-X and IBIS, the spectral fits of GRO J1008–57 in revolution 785 give a cutoff energy of ~ 13 keV, which is much lower than the derived cutoff energies of $\sim 23 - 29$ keV in the other five revolutions, so GRO J1008–57 showed a relatively soft spectrum in the early phase of the outburst. For three revolutions (203, 786 and 788) with a higher hard X-ray flux of $> \sim 10^{-9}$ erg cm $^{-2}$ s $^{-1}$ (X-ray luminosity of $\sim 3 \times 10^{36}$ erg s $^{-1}$ given a distance of 5 kpc) in the range of 3–100 keV (see Table 3), the additional absorption component below 5 keV is needed in the spectral fits. The large values for the column density of $\sim 5 \times 10^{22}$ cm $^{-2}$ suggest enhanced wind density near the periastron passage of the neutron star.

We also try to search for possible CRSFs in the hard X-ray spectra of GRO J1008–57 during the outbursts. In the energy range 10–60 keV, no absorption features are discovered in the spectra of GRO J1008–57. In two observational revolutions near the light curve peaks of two outbursts (revolution 203 in 2004 June and revolution 788 in 2009 March), we find the possible absorption line features around 70–80 keV in the residuals (the top two panels in Fig. 9). This absorption line feature is similar to the previously reported CRSF at 76 keV by MAXI/GSC observations (Yamamoto et al. 2013). Thus we have used the XSPEC model *cyclabs* to fit the possible CRSFs. The derived line parameters are presented in Table 3. For revolution 203, the CRSF is not significantly detected ($< 2\sigma$). The centroid energy of the line is derived around 74 keV, but the line width and depth can only be given with upper limits. For revolution 788, the CRSF is determined at the energy of $\sim 73.4 \pm 3.1$ keV, with a width of $\sim 2.6 \pm 1.9$ keV and a depth of $\sim 1.7 \pm 0.8$. The significance level of the detection for this cyclotron absorption feature is not yet so high (below 3σ , also comparing the reduced χ^2 for the different fits by no CRSF and with CRSF in Table 3), so we only report a marginal detection of the CRSF at ~ 74 keV in the GRO J1008–57 during the outburst with INTEGRAL. Our

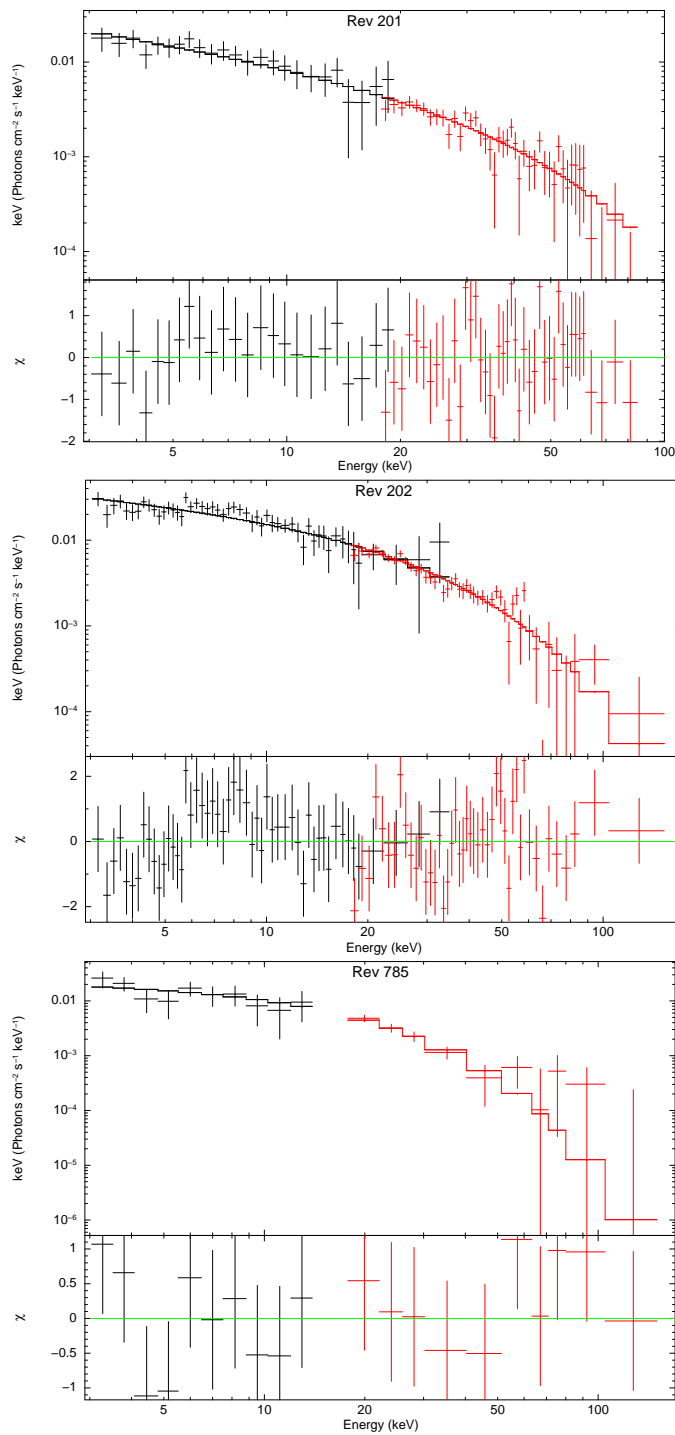


Fig. 8 The hard X-ray spectra of GRO J1008–57 during the outburst states obtained by JEMX and IBIS in three different observational revolutions (also see Table 3). The spectra for revolutions 201, 202 and 785 are fitted by a power-law plus high-energy exponential rolloff (*cutoffpl*). For revolution 786, an additional photoelectric absorption is added to fit the spectra below 5 keV.

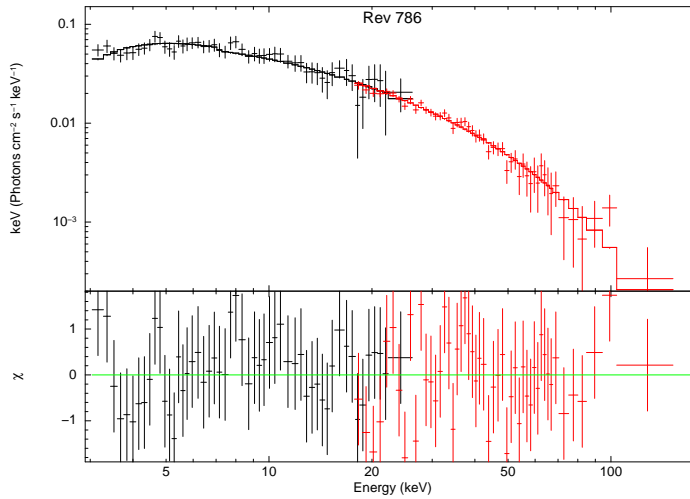


Fig. 8 — *Continued.*

results should still be consistent with the report by the MAXI/GSC observations (Yamamoto et al. 2013). Further observations of GRO J1008–57 with high sensitivity and high resolution during the outbursts are still needed in hard X-ray bands.

5 SUMMARY AND DISCUSSION

In this work, we analyzed variations in the spin period and spectral properties of the transient source GRO J1008–57 during the outbursts in 2004 June and 2009 March with INTEGRAL. We derived the spin period of GRO J1008–57 to be ~ 93.66 s in 2004 June and ~ 93.73 s in 2009 March. Combined with previous measurements of spin period, we find that the source has undergone a long-term spin-down trend since its discovery in 1993 to 2009 with a spin-down rate of $\sim 4.1 \times 10^{-5} \text{ s d}^{-1}$, and this might have changed to a long-term spin-up trend from 2009 to now. The hard X-ray spectrum of GRO J1008–57 during the outbursts can be well described by a cutoff power-law model, with a mean photon index of ~ 1.4 and cutoff energies of $\sim 23 - 29$ keV. For revolution 785 when GRO J1008–57 was in the early phase of the 2009 March outburst, the spectrum is softer than those around the outburst peaks, making GRO J1008–57 a weak hard X-ray source in IBIS detections. It is also interesting that IBIS and JEM-X detected GRO J1008–57 during its quiescence just before the outburst in 2009. The quiescent spectrum can be fitted to a simple power-law model with a photon index of ~ 2.1 , which is generally harder than the average spectra of accreting pulsars. In addition, above a hard X-ray flux of $\sim 10^{-9} \text{ erg cm}^{-2} \text{ s}^{-1}$ in the energy bands 3–100 keV, additional hydrogen absorption below 5 keV is needed, implying an enhanced wind density.

The pulse profiles of GRO J1008–57 during the outbursts were studied up to 70 keV in this work, and these are energy dependent: a double-peaked profile in the low energy band of 3–7 keV, and a single-peaked profile in hard X-ray bands (above 7 keV). These energy dependent pulse profile features are also detected in other Be transient X-ray pulsars, like A0535+262 (Naik et al. 2008) and 4U 0115+63 (Li et al. 2012). The double-peaked pulse profile features (or the dip-like structure) in the soft X-ray bands can be attributed to the obscuration of radiation by matter, as suggested in other Be/X-ray pulsars, so the observed dip-like feature in the pulse profile of GRO J1008–57 will be due to the additional absorption (instead of the Galactic column density) at the pulse phase. This idea is supported by our spectral analysis results of GRO J1008–57 around the peaks of the burst (see Table 3). The intrinsic absorption of $N_{\text{H}} \sim 6 \times 10^{22} \text{ cm}^{-2}$ is required in the spectral fits.

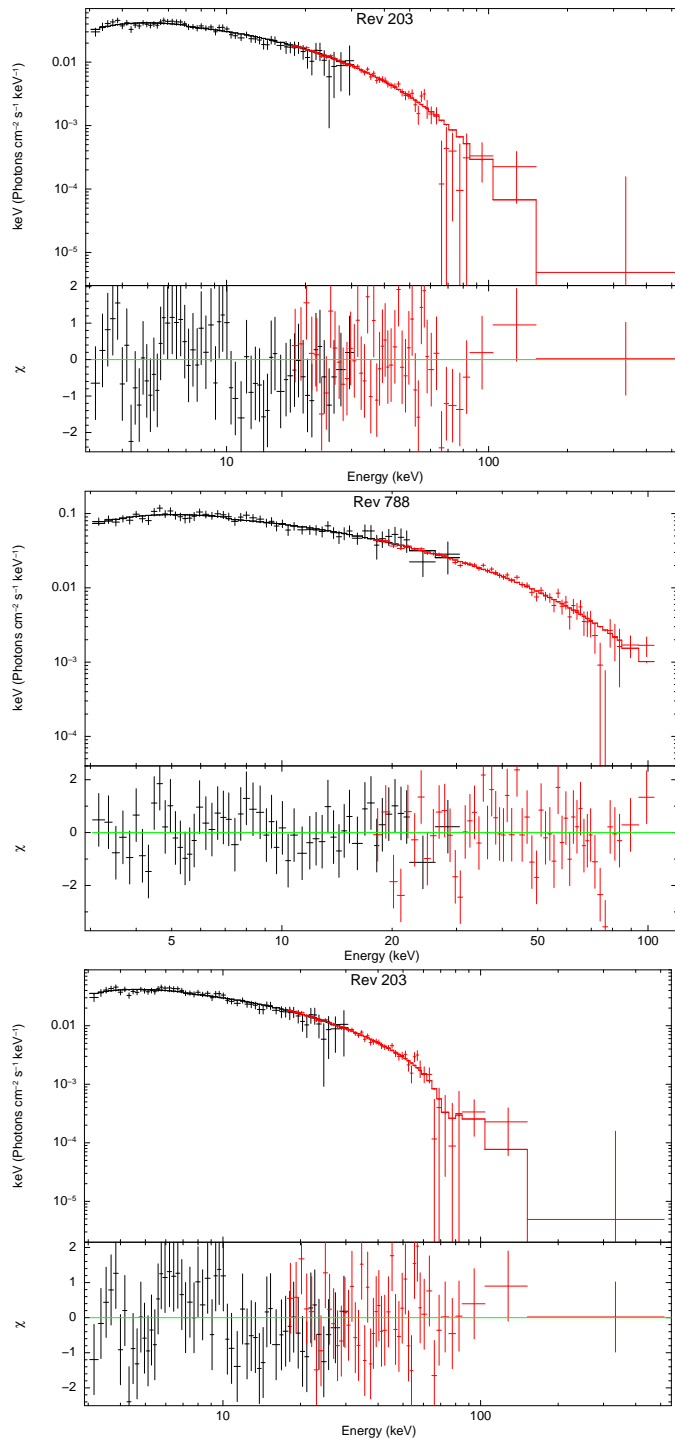


Fig. 9 The hard X-ray spectra of GRO J1008–57 around two outburst peaks: revolutions 203 and 788. The spectra are fitted by an absorbed power-law plus high energy exponential rolloff (*top two panels*), and the continuum model plus a possible CRSF around 74 keV (*the third and fourth panels*).

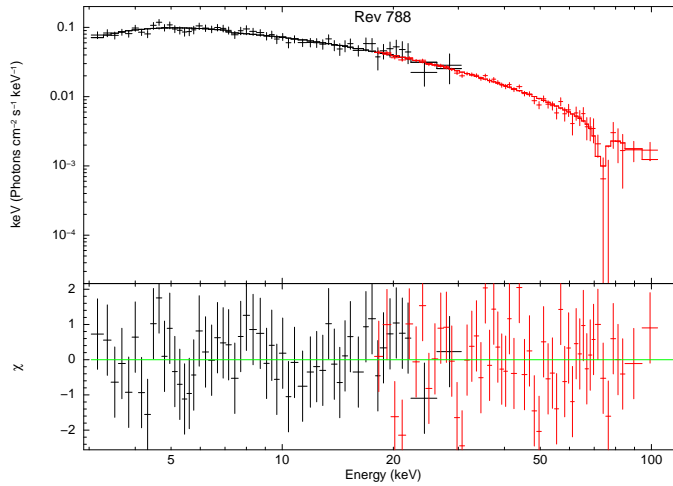


Fig. 9 — *Continued.*

With the RXTE/ASM data from 1996–2011, we analyzed the orbital modulation properties of GRO J1008–57, and found two modulation periods at 124.38 d and 248.78 d from the light curves in bands 1.5–12 keV. The orbital period should be 248.78 d, but what are implications for the modulation period of 124.38 d? Generally, an equatorial circumstellar disk exists around the companion star in Be/X-ray pulsar systems. Normal type I outbursts occur near the periastron passage through the disk of the Be star, and the Be/X-ray pulsar system will be in quiescence in the other orbital phase. Then, two possible flares could occur when the neutron star passes through the disk twice in one orbit. This idea is supported by the folded orbital light curve (Fig. 6). Two flare peaks appear in the folded light curve of the ASM data: one outburst peak in hard X-rays, with a harder spectrum that may even disappear in the low energy band < 3 keV; and a second flare peak separated by half of the orbital phase that shows a very soft spectrum and cannot be observed above 5 keV. The INTEGRAL spectral analysis on GRO J1008–57 during the outburst has suggested enhanced hydrogen absorption near the periastron passage. The hard spectrum during the outburst is mainly caused by strong absorption in the soft X-ray bands. However, the second flare near the apastron passage with a very soft spectrum can only be detected in soft X-rays, so this is the reason that hard X-ray detectors like BATSE, Swift, INTEGRAL and Suzaku can only detect the 248-day orbital modulation. The suggested equatorial circumstellar disk near the apastron passage of the neutron star has a much lower hydrogen density than that of the periastron passage, so the low accretion rate onto the surface of the neutron star will produce a thermal spectrum with a typical temperature of ~ 1 keV and this thermal spectrum cannot be strongly affected by absorption because of the low hydrogen density near apastron. This double disk-passage scenario is also suggested to explain the two modulation periods found in three other high-mass X-ray binaries: a Be/neutron star binary GRO J2058+42 (Corbet et al. 1997), a supergiant system 4U 1907+09 (Marshall & Ricketts 1980) and a peculiar main-sequence companion X-ray binary 4U 2206+54 (Wang 2009). Now, GRO J1008–57 becomes the second case of a Be/X-ray pulsar system with two periodic X-ray flares in one orbital phase. Why does the second peak show a very soft spectrum and what are the spectral characteristics of flares near the neutron star’s apastron passage? These issues need further work that would require follow-up observations by soft X-ray telescopes like Chandra and XMM-Newton.

Near the peak flux of the outburst, the possible 74 keV absorption line feature is detected in the hard X-ray spectrum of GRO J1008–57 by INTEGRAL. The present detection is still marginal, with a significance level of $\sim 3\sigma$. Our detection is also consistent with independent measurements reported by MAXI/GSC. In addition, we find that the derived fundamental line energy and cutoff en-

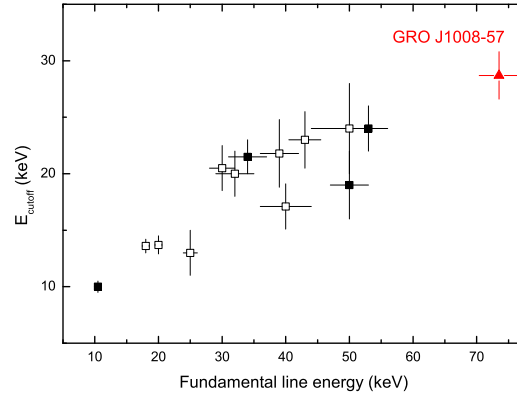


Fig. 10 The centroid energy of the fundamental cyclotron absorption line versus the cutoff energy (using a power law with an exponential high energy cutoff model) detected in accreting X-ray pulsar systems. A strong correlation exists between the line energy and cutoff energy, suggesting that the spectral cutoff in accreting X-ray pulsars is mainly caused by the cyclotron resonance (Coburn et al. 2002). The solid squares denote the Be/X-ray pulsars, and the hollow ones are other X-ray pulsar systems. These data points are collected from published literature, i.e., Be/X-ray pulsars: 4U 0115+63 (Li et al. 2012), 1A 1118-61 (Suchy et al. 2011), GX 304-1 (Klochkov et al. 2012), XTE J1946+274 (Coburn et al. 2002); another X-ray pulsar: 4U 1909+07 (Jaisawal et al. 2013), and others from Coburn et al. (2002). We also add the data point of GRO J1008–57 measured by INTEGRAL in the diagram. GRO J1008–57 follows the correlation well with the derived $E_c \sim 73.4$ keV and $E_{\text{cutoff}} \sim 28.7$ keV by INTEGRAL in revolution 788.

ergy in GRO J1008–57 by INTEGRAL are consistent with the relationship between the fundamental line energy and cutoff energy found in accreting X-ray pulsar systems.

In Figure 10, we collected the previous observational data with cyclotron line detections and high energy cutoff measurements in accreting X-ray pulsars, and plotted a diagram of fundamental line energy versus cutoff energy. The data point of GRO J1008–57 is also plotted, which is located in the upper panel of the correlation between the E_c and E_{cutoff} . This consistency also implies there is a cyclotron line feature at ~ 74 keV in GRO J1008–57, so GRO J1008–57 is the magnetized neutron star with the largest fundamental cyclotron energy (highest magnetic field due to electron absorption calculation) among known accreting X-ray pulsars.

The long-term variation in spin period of GRO J1008–57 was discovered in observations from different missions from the 1990s to 2012. From Figure 4, a spin-down trend dominates the spin evolution of the source from the 1990s to 2009. Generally, this fast, long-term spin-down trend is thought to be evidence for the propeller effect, which removes angular momentum from the neutron star by the interaction between matter and the magnetosphere (Illarionov & Sunyaev 1975; Bildsten et al. 1997). In the propeller phase of neutron star binaries, the spin-down rate can be estimated by the formula (Illarionov & Sunyaev 1975)

$$\dot{P} = \frac{10\pi\mu^2}{GM^2R^2}, \quad (1)$$

where $\mu = BR^3/2$, B is the surface magnetic field of the neutron star, M is the mass of the neutron star and R is the radius of the neutron star. If we take $M = 1.4 M_\odot$, $R = 10$ km and $\dot{P} = 4.1 \times 10^{-5} \text{ s d}^{-1}$, the derived surface magnetic field is $B = 6.2 \times 10^{12}$ G. This magnitude of the magnetic field is consistent with the derived strength from the cyclotron absorption line. It is quite interesting

that after 2009, maybe some time around 2009–2011, the neutron star in GRO J1008–57 changed into a spin-up trend. The spin-up rate was very large, almost $2 \times 10^{-4} \text{ s d}^{-1}$ from 2011 to 2012. What is the mechanism driving the reversal of accretion torque in Be/X-ray pulsars? We do not understand it yet. In some wind-fed supergiant X-ray binaries, this effect of reversal in accretion torque has also been observed (Bildsten et al. 1997). Thus torque reversal may be a common phenomenon in neutron star binaries, independent of the types of companion or accretion channels. In the early 1990s, GRO J1008–57 may have undergone a spin-up trend (from 1993–1996, as shown in Figure 4), but the number of data points are small. Now or in the future, we can still monitor the Be/X-ray pulsar GRO J1008–57 with INTEGRAL, Swift or Suzaku, studying the spin evolution, and in particular confirming the present spin-up trend. Studying GRO J1008–57 would help us to understand the physics of accretion torque reversal, and resolve the mystery of accretion in neutron star binaries.

Acknowledgements We are grateful to the referee for the fruitful suggestions that improved the manuscript. This paper is based on observations of INTEGRAL, an ESA project, with the instruments and science data center funded by ESA member states. We also used the archived data from RXTE/ASM on the ASM website provided by MIT. This work is supported by the National Natural Science Foundation of China (Grant No. 11073030).

References

- Bildsten, L., Chakrabarty, D., Chiu, J., et al. 1997, *ApJS*, 113, 367
Bird, A. J., Bazzano, A., Bassani, L., et al. 2010, *ApJS*, 186, 1
Coburn, W., Heindl, W. A., Rothschild, R. E., et al. 2002, *ApJ*, 580, 394
Coe, M. J., Roche, P., Everall, C., et al. 1994, *MNRAS*, 270, L57
Coe, M. J., Bird, A. J., Hill, A. B., et al. 2007, *MNRAS*, 378, 1427
Corbet, R., Peele, A., & Remillard, R. 1997, *IAU Circ.*, 6556, 3
Goldwurm, A., David, P., Foschini, L., et al. 2003, *A&A*, 411, L223
Illarionov, A. F., & Sunyaev, R. A. 1975, *A&A*, 39, 185
Jaisawal, G. K., Naik, S., & Paul, B. 2013, *ApJ*, 779, 54
Jourdain, E., Götz, D., Westergaard, N. J., Natalucci, L., & Roques, J. P. 2008, in *Proceedings of the 7th INTEGRAL Workshop*, Online at <http://pos.sissa.it/cgi-bin/reader/conf.cgi?confid=67>, 144
Klochkov, D., Doroshenko, V., Santangelo, A., et al. 2012, *A&A*, 542, L28
Kühnel, M., Müller, S., Kreykenbohm, I., et al. 2013, *A&A*, 555, A95
Lebrun, F., Leray, J. P., Lavocat, P., et al. 2003, *A&A*, 411, L141
Levine, A. M., & Corbet, R. 2006, *The Astronomer's Telegram*, 940, 1
Li, J., Wang, W., & Zhao, Y. 2012, *MNRAS*, 423, 2854
Lund, N., Budtz-Jørgensen, C., Westergaard, N. J., et al. 2003, *A&A*, 411, L231
Marshall, N., & Ricketts, M. J. 1980, *MNRAS*, 193, 7
Naik, S., Dotani, T., Terada, Y., et al. 2008, *ApJ*, 672, 516
Naik, S., Paul, B., Kachhara, C., & Vadawale, S. V. 2011, *MNRAS*, 413, 241
Petre, R., & Gehrels, N. 1994, *A&A*, 282, L33
Shrader, C. R., Sutaria, F. K., Singh, K. P., & Macomb, D. J. 1999, *ApJ*, 512, 920
Stollberg, M. T., Finger, M. H., Wilson, R. B., et al. 1993, *IAU Circ.*, 5836, 1
Suchy, S., Pottschmidt, K., Rothschild, R. E., et al. 2011, *ApJ*, 733, 15
Wang, W. 2009, *MNRAS*, 398, 1428
Wang, W. 2013, *MNRAS*, 432, 954
Yamamoto, T., Mihara, T., Sugizaki, M., et al. 2013, *The Astronomer's Telegram*, 4759, 1